Proceedings of Ninth World Conference on Earthquake Engineering
August 2-9, 1988, Tokyo-Kyoto, JAPAN (Vol.VIII)

SA-5

ESTIMATION OF STRONG GROUND MOTIONS IN MEXICO CITY

Hiroo KANAMORI[1], Paul C. JENNINGS[1], Donald HELMBERGER[1], Robert CLAYTON[2], J. Krishna SINGH[3], Luciana ASTIZ[4], and Enrique MENA[3]

[1]Professor, California Institute of Technology, USA
[2]Associate Professor, California Institute of Technology,USA
[3]Autonomous National University of Mexico, MEXICO
[4]Seismologist, California Institute of Technology, USA

SUMMARY

The authors report on simulations of ground motions in Mexico City expected for large earthquakes in the Guerrero seismic gap. The simulations use strong motion records of a recent M_S=5.8 earthquake in the Guerrero gap recorded in Mexico City as empirical Green's functions. For a range of earthquakes expected for the Guerrero gap, simulated ground motions are comparable to those recorded during the Michoacan earthquake.

1. Introduction

The Michoacan, Mexico, earthquake of September 19, 1985 (M_W=8.0) is the most damaging event to date in that country. Along the Mexican subduction zone, about ten earthquakes with M_S >7.5 have occurred during the past 60 years. The magnitudes of these events are almost comparable to the 1985 Michoacan earthquake, but none of them caused as much damage in Mexico City. Although many of the seismic gaps along the Mexican coast have been filled by large earthquakes during the last two decades, a prominent gap in Guerrero, about 250 km to the southeast of the Michoacan gap, has not broken since 1911 (Figure 1). The size of this gap is similar to that of the Michoacan gap.

In view of this situation, we performed a simulation of ground motions expected in Mexico City from a hypothetical earthquake in the Guerrero gap. This simulation is based on the source spectra of the Michoacan earthquake and other major events in Mexico.

2. 1985 Michoacan Earthquake

The 1985 Michoacan earthquake is well-studied (see, for example, the papers in Ref. 1). The earthquake has a low-angle thrust mechanism typical of Mexican subduction-zone earthquakes. The source consists of two major events about 90 km and 25 sec apart. Houston (Ref. 2) deconvolved body waves observed at many stations world-wide to obtain the fault rupture pattern in Figure 2. In this solution, the source consists of approximately 50 subevents with seismic moments ranging from 3x10**25 to 23x10**26 dyne-cm.

3. Method

The simulation method is similar to the one used by Kanamori (Ref. 3) and Hartzell (Ref. 4) and employs observed accelerograms as empirical Green's functions. In this study, we used strong motion accelerograms from small events in the Mexican coastal areas recorded in Mexico City as the empirical Green's functions. In addition we employed source scaling relations established for large subduction-zone earthquakes (Refs. 5 and 6) to approximate the ground motions from each sub-event shown in Figure 2.

Let $f_i(t-\tau_i;\ m_i)$ be the ground motion observed from the i-th subevent with seismic moment m_i and onset time τ_i. Then the total ground motion from N subevents is

$$s(t) = \sum_{i=1}^{N} f_i(t-\tau_i;\ m_i) \qquad (1)$$

We use the ground motion from a reference event $f_r(t;\ m_r)$ as the empirical Green's function. Then using a seismic scaling relation $T(\omega;\ m_i,\ m_r)$, we write

$$|\hat{f}_i(\omega;\ m_i)| = \hat{T}(\omega;\ m_i, m_r)\,|\hat{f}_r(\omega;\ m_r)|$$

where the accented variables are Fourier transforms. Houston and Kanamori (Ref. 7) showed that the following ω- square source model is a good approximation for 5 Mexican subduction-zone events.

$$\hat{M}(\omega) = M_0 \frac{\omega_c^2}{\omega^2+\omega_c^2} \qquad (2)$$

where the corner frequency ω_c is given by

$$\omega_c = 3.08\beta\left(\Delta\sigma/M_0\right)^{1/3} \qquad (3)$$

with stress parameter $\Delta\sigma$ = 30 bars and S-wave velocity β = 3.5 km/sec. Using (2), we obtain

$$\hat{T}(\omega;\ m_i, m_r) = \frac{m_i}{m_r}\,\frac{\omega_i^2}{\omega_r^2}\,\frac{\omega^2+\omega_r^2}{\omega^2+\omega_i^2} \qquad (4)$$

in which ω_r is the corner frequency of the reference event.

Assuming that the phase spectrum does not change with the event size, we can write the ground motion for the i-th event as

$$f_i(t-\tau_i;\ m_i) = \int_{-\infty}^{+\infty} e^{-i\omega\tau_i}\hat{T}(\omega;\ m_i, m_r)\ \hat{f}_r(\omega;\ m_r)e^{i\omega t}d\omega \qquad (5)$$

Since performing the transform (5) for all the subevents is time consuming, we perform the computation in the frequency domain. Taking the transform of (1) and using the above relations, we obtain

$$s(\omega) = \frac{\hat{f}_r(\omega;\ m_r)}{m_r\omega_r^2}\sum_{i=1}^{N}\frac{m_i\omega_i^2(\omega^2+\omega_r^2)}{\omega^2+\omega_i^2}e^{-i\omega\tau_i} \qquad (6)$$

We first compute $\hat{s}(\omega)$ using m_i, m_r, and τ_i(ω_i and ω_r are obtained from m_i and m_r using (3)), and inverse transform it obtain s(t). Note that the procedure uses no arbitrary scaling parameters.

4. Test of the Method.

We first tested our method for the Michoacan earthquake using strong ground motions from the two major aftershocks as the empirical Green's functions. Figure 3 shows the strong motion record of the Sept. 21, 1985, aftershock, the simulated ground motion, and the observed ground motion for the main shock. These are the E-W components at a lake-bed site (CDAO) in Mexico City. The velocity response spectra (5% damping) are shown in Figure 4. Although the waveform of the simulation differs in detail from the observed ground motion, the overall shapes of the waveform and the response spectrum are very similar to those observed.

Figures 5 and 6 show the results of simulation using a smaller aftershock (M_W = 6.9, April 30, 1986) as the Green's function. The spectral amplitude of the simulated motion peaks at a slightly lower period than the actual event, but the amplitudes and spectral shape agree reasonably well. The waveforms are more dissimilar than in the previous case.

5. Simulation for Events in the Guerrero Gap

5.1 Guerrero Gap

Because of uncertainties in defining the Guerrero gap, we will consider two models for the next Guerrero earthquake. The first model is similar to the 1985 Michoacan earthquake, and fills the entire gap between the 1979 event and the 1957 event. The second model follows the interpretation that the previous activity from 1899 and 1911 represents a sequence of events smaller than the 1985 event. Model 2 is an event which represents the first half of the Michoacan sequence (M_W=7.6).

5.2 Green's Function

On Feb. 8, 1988, an earthquake with M_S=5.8, near the northwestern edge of the Guerrero gap, was recorded by strong-motion seismographs in Mexico City (Figure 7). These records play a key role in this simulation because they include the path effect from the Guerrero gap to Mexico city and the site response. The location suggests that it is a typical subduction event.

5.3 Simulation

The results of simulation for Models 1 and 2 are shown in Figures 8 and 9. The simulated motion for the large earthquake of Model 1 (simulation 2) is enriched in short period energy in comparison to the 1985 Michoacan event. As Figure 9 shows, at periods shorter than 3 sec, the simulated motion is about 3 times larger than the Michoacan event. However, at periods longer than 3 sec, the Michoacan event has a larger spectral amplitude. The abundance of the short-period energy for the Guerrero event could be due to its shorter distance to Mexico City.

Since the rupture pattern of the Guerrero earthquake is not known, we tested the effect of rupture pattern by randomly moving the locations of the subevents in Figure 2 by ±20 km in both the strike and the down-dip directions. We also changed randomly their onset times by ±5 sec. This perturbation is large enough to change substantially the rupture pattern of the Michoacan earthquake. The results for this perturbed model are shown in Figures 8 and 9 (simulation 4). The amplitude of this simulated motion is about 30% smaller than simulation 2.

For the smaller event of Model 2, the simulated motion is about 1/3 of that for Model 1, and is significantly smaller than the ground motions for the Michoacan event at periods longer than 1 sec. (simulation 3). At periods shorter than 1 sec, the simulated motion is about a factor of 2 larger than the Michoacan event. The duration of ground motion is about half that of the Michoacan event, reflecting the smaller size of the fault plane.

6. Discussion and Conclusions

Our simulations indicate that if the Guerrero event is as large as the 1985 Michoacan event, the resulting ground motion in Mexico City will be comparable to that of the 1985 Michoacan earthquake at periods longer than 3 sec. At periods shorter than 3 sec, the amplitude will be 2 to 3 times larger than that for the Michoacan earthquake. If the expected Guerrero events occur as a sequence of magnitude 7.5 shocks, as they did in the previous sequence, the strong motion in Mexico City will be considerably smaller than that experienced during the 1985 Michoacan earthquake at periods longer than 1 sec, but stronger than the 1985 event at short periods. In either case, the level of motion indicated by the simulations would be potentially damaging to a wide range of structures.

Since the method involves established scaling relations and no free parameters, the results obtained here are considered robust. However, the results depend on the character of the event used as the Green's function, and upon the scaling relation used to determine the spectrum of subevents. In addition, the simulations depend upon the rupture pattern.

The scaling relation used is one of the simplest ones consistent with the Mexican subduction zone. Any other scaling relation that is consistent with the events in Mexico is expected to yield similar simulated ground motions. For example, a drastic change in the stress parameter $\Delta\sigma$ from 5 to 200 bars results in only a 15% change in the amplitude of simulated motion. Similarly, changes in the rupture pattern would not drastically change the characteristics of the simulated ground motion. The method is, however, more sensitive to the characteristics of the event used as a Green's function.

REFERENCES

1. Geophys. Res. Letters, 13, 1986.
2. Houston, H., "Source Characteristics of Large Earthquakes at Short Periods," Ph.D. Thesis, California Institute of Technology, Dec. 15, 1986.
3. Kanamori, H., "A Semi-Empirical Approach to Prediction of Long-Period Ground Motions from Great Earthquakes," Bull. Seismolol. Soc. Am., 69, 1645-1670, 1979.
4. Hartzell, S. H., "Earthquake Aftershocks as Green's Functions," Geophys. Res. Let., 5, 1-4, 1978.
5. Hartzell, S. H., and Heaton, T. H., "Teleseismic Time Functions for Large, Shallow Subduction Zone Earthquakes," Bull. Seismol. Soc. Am., 75, 965-1004, 1985.
6. Houston, H., and Kanamori, H., "Source Characteristics of the 1985 Michoacan, Mexico Earthquake at Periods of 1 to 30 Seconds," Geophys. Res. Lett., 13, 597-600, 1986.
7. Houston, H., and Kanamori, H., "Source Spectra of Great Earthquakes: Teleseismic Constraints on Rupture Process and Strong Motion, Bull. Seismol. Soc. Am., 76, 19-42, 1986.

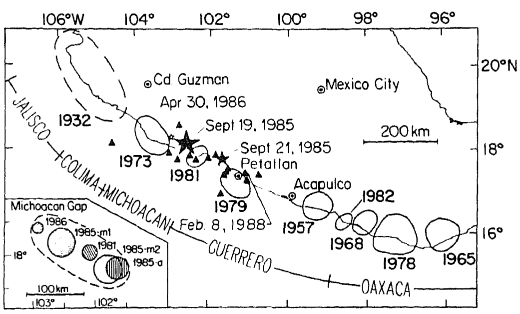

Fig. 1 Historic earthquakes and their aftershock areas for the southwest coast of Mexico.

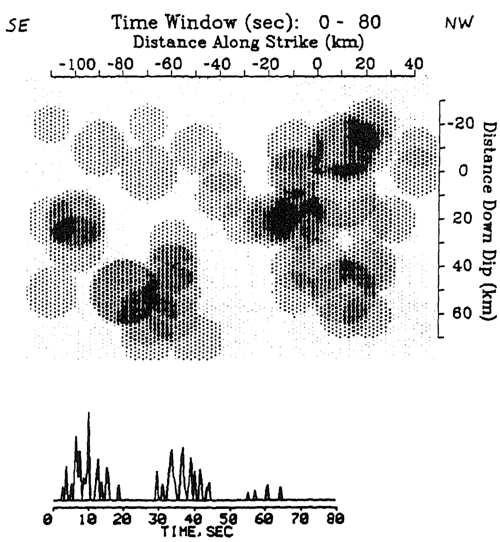

Fig. 2 (a) Spatial distribution of moment release for the 1985 Michoacan earthquake. The area of the circles approximates the rupture area of each source and the shading is proportional to the moment release per unit area.
(b) Timing of initiation of each point source of part a.

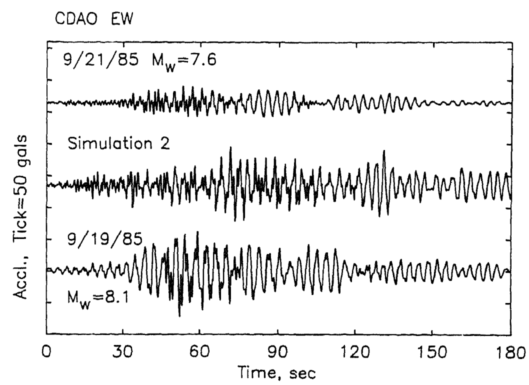

Fig. 3 Michoacan simulation at CDAO site using Sept. 21 aftershock as Green's function.

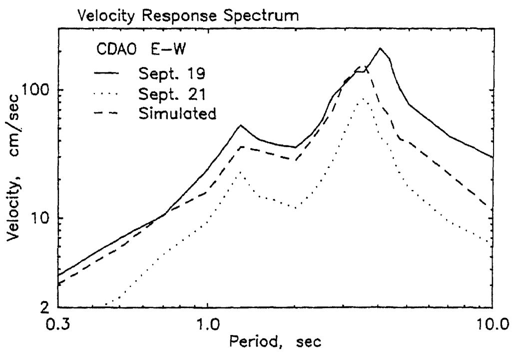

Fig. 4 5% damped response spectra of accelerograms from Fig. 3.

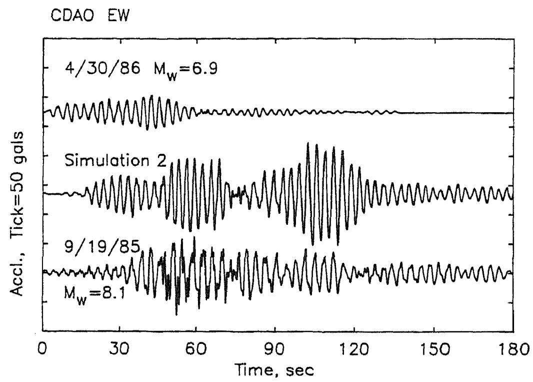

Fig. 5 Michoacan simulation at CDAO site using April 30 aftershock as Green's function.

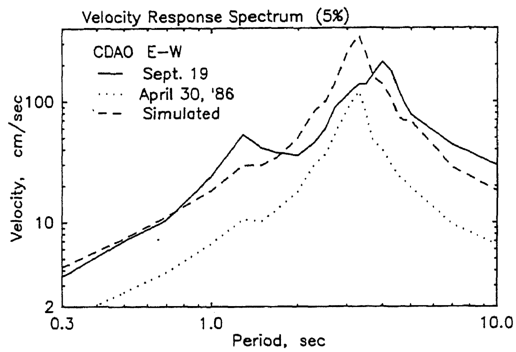

Fig. 6 5% damped response spectra of accelerograms from Fig. 5.

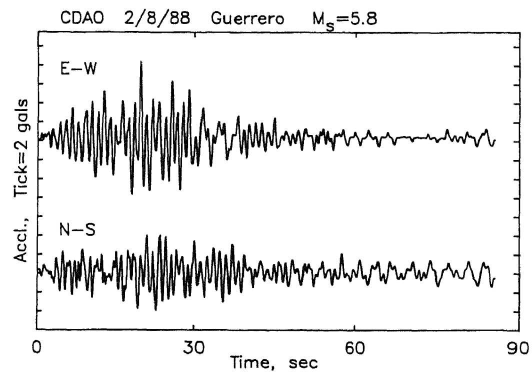

Fig. 7 Accelerogram of Feb. 8, 1988, Guerrero earthquake (M = 5.8) as recorded at CDAO site.

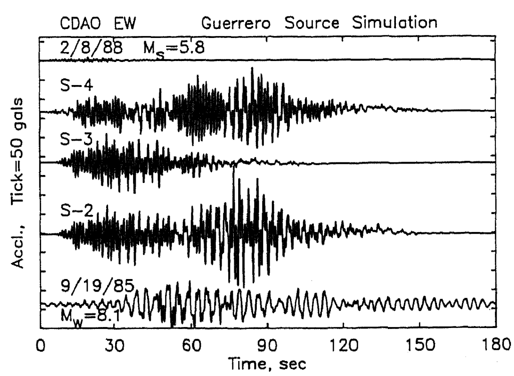

Fig. 8 Guerrero simulation at CDAO site using Feb. 8, 1988 accelerogram as Green's function.

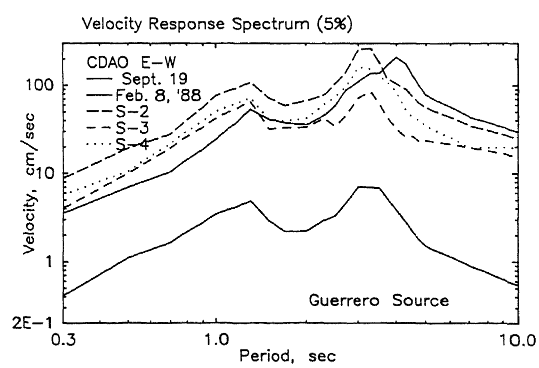

Fig. 9 5% damped response spectra of accelerograms shown in Fig. 8.